Optical manifestation of the Stoner ferromagnetic transition in two-dimensional electron systems

A. B. Van'kov,[1,2] B. D. Kaysin,[1] and I. V. Kukushkin[1,2]
[1]*Institute of Solid State Physics, RAS, Chernogolovka 142432, Russia*
[2]*National Research University Higher School of Economics, Laboratory for Condensed Matter Physics, Moscow 101000, Russia*
(Received 21 July 2017; revised manuscript received 15 October 2017; published 1 December 2017)

We perform a magneto-optical study of a two-dimensional electron systems in the regime of the Stoner ferromagnetic instability for even quantum Hall filling factors on $Mg_xZn_{1-x}O/ZnO$ heterostructures. Under conditions of Landau-level crossing, caused by enhanced spin susceptibility in combination with the tilting of the magnetic field, the transition between two rivaling phases, paramagnetic and ferromagnetic, is traced in terms of optical spectra reconstruction. Synchronous sharp transformations are observed both in the photoluminescence structure and parameters of collective excitations upon transition from paramagnetic to ferromagnetic ordering. Based on these measurements, a phase diagram is constructed in terms of the two-dimensional electron density and tilt angle of the magnetic field. Apart from stable paramagnetic and ferromagnetic phases, an instability region is found at intermediate parameters with the Stoner transition occurring at $\nu \approx 2$. The spin configuration in all cases is unambiguously determined by means of inelastic light scattering by spin-sensitive collective excitations. One indicator of the spin ordering is the intra-Landau-level spin exciton, which acquires a large spectral weight in the ferromagnetic phases. The other is an abrupt energy shift of the intersubband charge density excitation *due to reconstruction of the many-particle energy contribution*. From our analysis of photoluminescence and light scattering data, we estimate the ratio of surface areas occupied by the domains of the two phases in the vicinity of a transition point. In addition, the thermal smearing of a phase transition is characterized.

DOI: 10.1103/PhysRevB.96.235401

I. INTRODUCTION

Two-dimensional electron systems (2DES) with strong interaction have attracted considerable research attention from the perspective of fundamental physics. The technological perfection of novel 2D materials extends their parameter space far beyond the framework of GaAs-based heterostructures. Interesting examples include 2D Fermi liquids in ZnO-based heterostructures, which exhibit an unusual combination of a large value of the interaction parameter (Wigner-Seitz radius) r_s with ultrahigh electron mobility level [1,2]. New correlated states in magnetic fields may appear as a result of the interplay between key energy scales: cyclotron, Zeeman splitting, and interparticle Coulomb energy. The material parameters of ZnO-based structures with 2DES facilitate close proportion between energy scales in magnetic fields: Zeeman splitting ($g^*_{\text{bulk}} \sim 2$) and cyclotron energy ($m^*_{\text{bulk}} \sim 0.28\, m_0$). At moderate magnetic fields, the Coulomb energy has a substantially higher scale, thus resulting in considerable Landau-level (LL) mixing and entangling the familiar single-particle energy spectrum. Nevertheless, the energy-level sequence may be partially restored if renormalization of Fermi-liquid parameters is taken into account. In this context, in previous works, a substantial renormalization of the electron effective mass and spin susceptibility has been observed in ZnO at large values of the interaction parameter r_s [3–5]. As a result, opposing spin levels of adjacent LLs may approach closer to each other in terms of energy than those of the same LL. If they happen to intersect, spontaneous symmetry breaking between two rivaling spin configurations is possible. At integer Landau-level fillings, the corresponding phases are called quantum Hall ferromagnets (QHFs) and can be treated within the confines of the Ising model. Experimentally, this Ising ferromagnetic (FM) transition is triggered either by tuning the electron's spin susceptibility, or if the spin splitting is not sufficiently large, by tilting the external magnetic field at definite *coincidence* angles.

The appropriate coincidence angles can be estimated from the following simplified single-particle relation:

$$\frac{E_z}{\hbar\omega_c} = \frac{g^* m^*}{2\cos\Theta} = j, \tag{1}$$

where g^*m^* represents the effective spin susceptibility, Θ the tilt angle of the magnetic field, and integer j the coincidence index. This formula has been regularly utilized in magnetotransport experiments for probing the spin susceptibility, but for systems with strong interaction this parameter can be significantly renormalized. Applicability of Eq. (1) at small integer or fractional filling factors may be violated due to the strong exchange effects, which lead to modification of the energy spectrum [5,6]. The physics of fractional quantum Hall states may be also modified by level crossing, though in this case levels of composite fermions play the role. In particular, certain unknown even-denominator fractional states have been detected in ZnO-based 2DES [6] at tilt angles different from single-particle values obtained from Eq. (1).

The physics of Ising QHFs at small integer filling factors is essentially a many-body problem since it is governed by the exchange interaction. As has been established earlier in a series of magnetotransport studies of 2DESs in different heterostructures [7–10], a Stoner ferromagnetic transition at integer filling factors involves the formation of domains. The transition point has been identified in all those cases and later in ZnO-based heterostuctures [4,6] by the appearance of sharp resistance spikes due to the scattering on domain walls. Nevertheless, important physical parameters such as the energy spectrum of the different phases, areas occupied by them, and the stability of domains remained unknown.

TABLE I. Parameters of two-dimensional electron system (2DES) in the set of studied samples in order of increasing electron density. The electron density n_s was measured using the magnetophotoluminescence technique. Mobility μ_t was qualified by magnetotransport measurements.

Sample ID	n_s (10^{11} cm^{-2})	μ_t (10^3 cm^2/V s)
254	1.14	710
259	1.8	570
244	2.3	400
427	2.8	427
426	3.5	410
448	4.5	250

In this context, here, we present an optical study of a Stoner ferromagnetic transition in a set of ZnO-based heterostructures with 2DESs in the regime corresponding to the integer quantum Hall effect. Transformations of the $\nu = 2$ ground state are carefully studied, and consonant events for other filling factors of 3, 4, and 6 were also traced. The conditions for a Stoner transition are determined in view of abrupt transformations in the 2DES energy spectra. Qualitative reconstruction is detected both in the magnetophotoluminescence (magneto-PL) spectrum and parameters of the electronic collective excitations, as probed by inelastic light scattering (or the Raman) technique. The phase diagram of Ising QH ferromagnets at $\nu = 2$ is acquired in terms of the critical tilt angle as a function of the electron density. Three essential regions are identified in the diagrams: stable paramagnetic (PM) region, FM region, and an instability region, wherein the Stoner transition takes place at $\nu = 2$ or in the vicinity. At electron densities of $n_s < 2 \times 10^{11}$ cm^{-2}, FM order is observed to spontaneously develop even at normal orientation of the magnetic field. The spin polarization of the phases is probed via Raman scattering on the intra-Landau-level spin exciton. From an analysis of the PL and Raman spectra, the ratio of areas occupied by the domains of the two rivaling phases across the transition point is estimated. Furthermore, the domain sizes and their thermal stability are probed.

II. EXPERIMENTAL TECHNIQUE

Measurements were performed on a series of $Mg_xZn_{1-x}O/ZnO$ heterostructures grown by liquid-ozone-assisted molecular beam epitaxy [1]. Each structure contained a high-quality 2D electron channel of varying density, as defined by the Mg content in the barrier. Key parameters of the as-grown samples were characterized by magnetotransport analysis and are summarized in Table I.

Experiments were conducted at low temperatures in the range of 0.3–4.2 K using the He^3 evaporation inset to the cryostat with a superconducting solenoid. Samples were mounted on a rotational stage in order to control their orientation with respect to the magnetic field direction. Tilt angles were tuned *in situ* with discrete steps with a finesse of $\sim 0.5^\circ$. The applied magnetic fields spanned the range of 0 to 15 T.

Optical access to the sample was established via two quartz fibers, one of which was used for photoexcitation, while the other was used for signal collection. This optical scheme benefits from a higher signal output and the absence of background parasitic scattering from the fiber core. The angle configuration of the fibers determined the momentum transferred from light to the 2DES. Photoexcitation was produced by a tunable laser source operating in the vicinity of the direct interband optical transitions of ZnO. The laser source was designed as a frequency-doubled tunable continuous-wave Ti:sapphire laser with output monochromatic radiation in the wavelength range of 365 to 368 nm. A barium borate crystal set in the single-pass configuration was utilized as a nonlinear element. The typical UV excitation power was 2–7 μW, which was distributed over an excitation spot with a surface area ~ 1 mm^2. Thus, the excitation power density was well below 1 mW/cm^2, and which prevented the heating of 2D electrons. Optical spectra were detected with the use of a spectrometer in conjunction with a liquid-nitrogen-cooled CCD camera. In the UV range, the system exhibited a linear dispersion of 5 Å/mm and spectral resolution of 0.2 Å.

The optical response of each sample was studied with respect to the magnetic-field orientation in order to study the recombination spectrum transformation in the vicinity of integer filling factors. In addition, PL was utilized for electron density characterization, as described previously [11], and for determining the resonant conditions of inelastic light scattering.

Inelastic light scattering signal was studied predominantly at magnetic fields corresponding to LL filling factors of $\nu = 2$, $\nu = 1$, and values in-between. The multitude of spectral lines was dominated by a PL signal residing at stationary wavelength positions, and it was not affected by laser tuning. Raman lines, although weak, could be distinguished by their constant energy shift from the sweeping laser position. An important observation here is that the intensities of the Raman features from 2D electrons behave resonantly while crossing definite PL bands. This trick has been thoroughly described in the previous paper, devoted to collective excitations in ZnO-based 2DESs at zero magnetic field [12]. Here, at high magnetic fields, the Raman line search procedure was essentially the same as in the previous study, and only the resonant contours were slightly shifted by the applied magnetic field.

III. OPTICAL RESPONSE OF QUANTUM HALL FERROMAGNETS

The first indication of the rearrangement in LLs is manifested in *the modification of the magnetic-field dependence of photoluminescence*. Figures 1(a)–1(c) present the PL evolution of the 2DES in Sample 427 (density $n_s = 2.8 \times 10^{11}$ cm^{-2}) as image plots with the magnetic field increasing along the downward y direction. The evolution of PL spectra shown in Fig. 1(a) ($\Theta = 25^\circ$) and those at smaller angles are all nearly equivalent if corrected to the normal component of the magnetic field. They represent smooth $1/B_\perp$-periodic oscillations of the PL intensity at spectral positions close to the Fermi level as the 2DES transitions through conventional quantum Hall states [11]. Note that despite its obvious 2D nature, the magnetic-field evolution of PL features on Fig. 1(a) hardly resembles the familiar fan of Landau levels. The picture is especially complicated for samples with small electron densities, where the interaction parameter $r_s \gg 1$

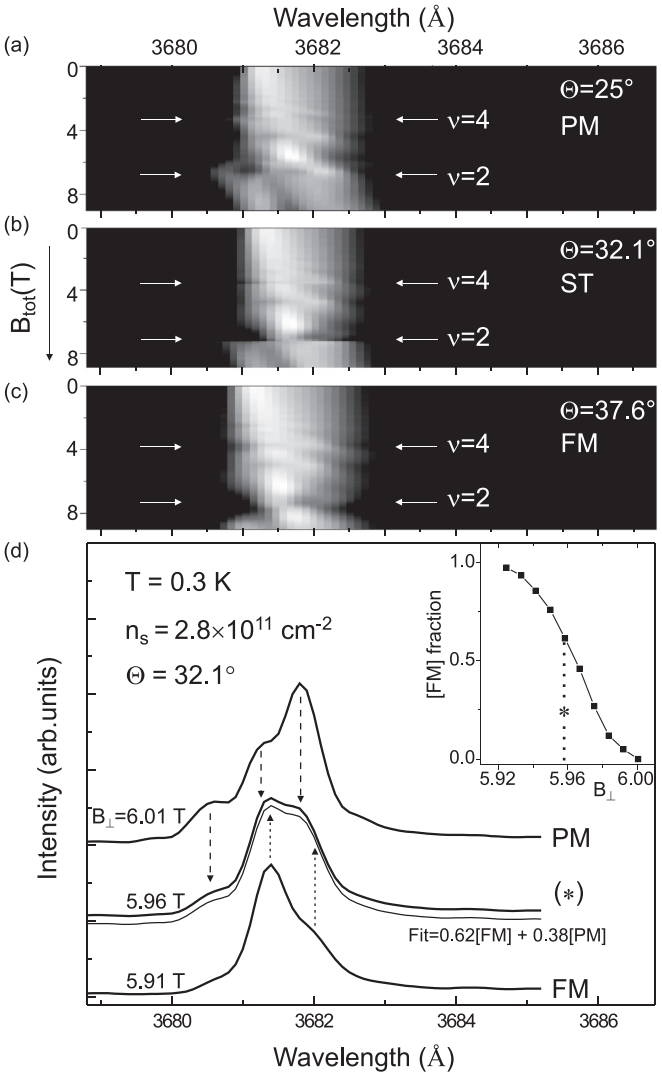

FIG. 1. (a)–(c) Image plots of the magnetic-field dependence of photoluminescence (PL) of the 2DES in MgZnO/ZnO heterostructure with $n_s = 2.8 \times 10^{11}$ cm^{-2} measured at three sample orientations Θ, corresponding to qualitatively different behaviors at even filling factors: (a) paramagnetic, (b) Stoner transition, and (c) ferromagnetic ordering. Positions with distinctive PL behavior at $\nu \approx 2$ and 4 are indicated by double horizontal arrows. In panel (b), *PL jump positions* are discernible by image discontinuity. (d) Modification of PL spectra across the Stoner transition region, while fine tuning the magnetic field at the fixed tilt angle 32.1°. The three spectra correspond to ferromagnetic, paramagnetic phases and their superposition at the intermediate field point. In all cases, the temperature of the sample was close to 0.3 K. The inset illustrates a fraction of the ferromagnetic phase as a function of the magnetic field *across the transition region*, as extracted from the superposition fit. The asterisk marks *the critical field, corresponding to PL jump position*.

($r_s \approx 7$ for the Sample 427 with $n_s = 2.8 \times 10^{11}$ cm^{-2}). This entanglement of the magneto-PL evolution is likely due to the strong Landau-level mixing. In particular, the number of recombination peaks at $\nu = 2$ exceeds that of nominally filled electron spin levels [see the top spectrum on Fig. 1(d)].

On further tilting of the field, we observe a qualitatively different behavior: *the evolution of spectra* undergoes abrupt transformations at *some critical* magnetic field values close to filling factors $\nu = 2$, 4, 6 [see Fig. 1(b)]. In particular, on the high-field side of this *critical field* near $\nu = 2$, the PL evolution coincides with the previous case of Fig. 1(a), but at smaller fields, the spectrum undergoes a sudden "reorganization": two peaks emerge instead of three, and their oscillator strengths become inverted [see top and bottom spectra in Fig. 1(d)]. The high-energy spectral line centered at ~3680.5 Å for $\nu = 2$ and also developed at other even filling factors completely disappears [compare Fig. 1(c) with Fig. 1(a)]. This reconstruction (or jump) of the PL spectrum is indicative of the abrupt magnetic-field-driven change in the ground state. The PL jump is observed within some range of the *critical* tilt angles at definite *critical* filling factor values. At even greater angles, the magnetic-field dependence eventually becomes "smooth" again with the modified PL spectrum near even filling factors [see Fig. 1(c)]. This new appearance of spectra at even filling factors is identical to those at $B < B^*$ near the PL jump [the lowest spectrum on Fig. 1(d)] and thus represents the PL signature of the new phase developed nearby $\nu = 2$. At critical angles supporting abrupt PL transformations, the 2DES undergoes a phase transition. As discussed below and in accordance with previous magnetotransport results [4,6], the two phases nearby $\nu = 2$ correspond to paramagnetic ordering with opposite LL spin states equally occupied and ferromagnetic ordering with inverted spin orientation of the highest occupied spin level. For the sake of brevity, the PL spectra of different phases in Fig. 1 are denoted as PM and FM.

An interesting interplay between the two phases can be observed across the narrow B-field transition region. Here, the resulting spectrum is composed of the superposition of the PM and FM spectra [Fig. 1(d)]. The proportion between the phases is gradually switched from the full PM to the full FM state over a span of $\Delta B \sim 0.1$ T. An example of the best linear superposition fitting the mixed PL spectrum is overlaid on the middle spectrum in Fig. 1(d), and the relative weights are plotted for the relevant range of magnetic fields in the inset therein. This system state witnesses the coexistence of domains in a narrow transition region of magnetic fields and facilitates direct estimation of the phase percentage. Analogous interplay between the two phases has been detected while tuning the tilt angle at the fixed filling factor $\nu = 2$. Figure 2 shows the waterfall of spectra at five closely spaced angles in the range, where PM-FM transition occurs. The evolution of the fraction of the FM phase, as extracted from the linear superposition fit, is plotted as a function of the angle Θ in the inset to Fig. 2. It is reasonable to take the position of the half-height as the critical angle Θ^* for the transition at $\nu = 2$.

Similar experiments were performed on all other samples listed in Table I with electron densities ranging from 1.14×10^{11} to 4.5×10^{11} cm^{-2}. The data are consolidated on a plot with critical angles as a function of the electron density (Fig. 3). For samples with densities exceeding 2×10^{11} cm^{-2}, this diagram includes three regions with qualitatively different magneto-PL behavior around even filling factors. At a number of tilt angles (shown as gray symbols) the Stoner instability was recognized as PL jumps at some critical filling factors $\nu^* \approx 2$. Singularities at $\nu \approx 4$ and 6 appeared with somewhat weaker contrast. Stable PM and FM phases in vicinity of $\nu = 2$ are seen at angles respectively smaller and larger than

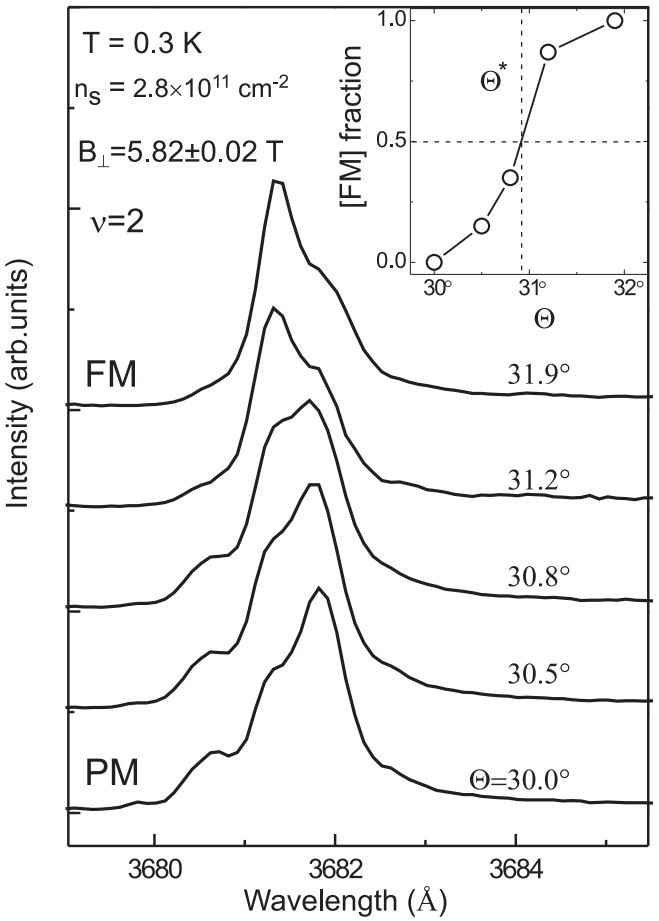

FIG. 2. The waterfall of PL spectra, recorded at $\nu = 2$ on the sample with density $n_s = 2.8 \times 10^{11}$ cm^{-2}, with the magnetic-field tilt angle Θ gradually tuned across the Stoner transition. At smaller angles, the signal from paramagnetic phase (PM) dominates, conversely ferromagnetic phase (FM) prevails at higher angles. The inset illustrates a fraction of the ferromagnetic phase as a function of the tilt angle at $\nu = 2$, as extracted from the superposition fit. The Θ^* marks the tilt angle of the Stoner transition at $\nu = 2$.

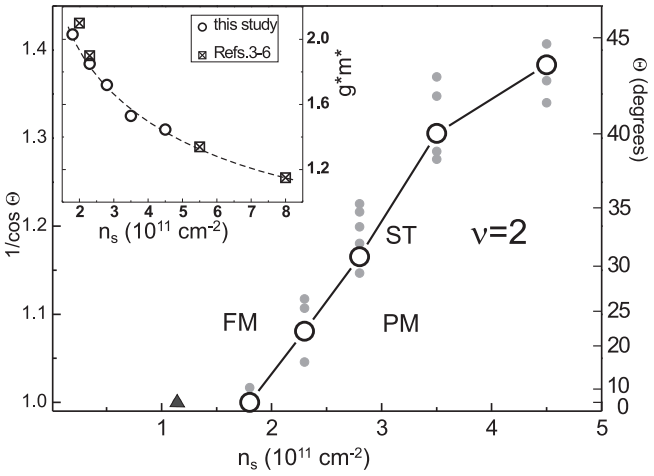

FIG. 3. Phase diagram of Ising quantum Hall ferromagnets at $\nu = 2$, obtained as a plot of the critical tilt angle versus electron density. Open black circles correspond to tilt angles, supporting the Stoner transition (ST) at $\nu = 2$. Ranges corresponding to ferromagnetic and paramagnetic phases at $\nu = 2$ are above and below the black curve. For all samples except the lowest density one, few other tilt angles, at which the Stoner instability is detected at $\nu <$ or > 2 are also shown with gray symbols. For the lowest density sample with $n_s = 1.14 \times 10^{11}$ cm^{-2}, the Stoner ferromagnet at $\nu = 2$ is observed already at normal magnetic-field orientation (triangle symbol). The inset illustrates the electron density dependence of the enhanced spin susceptibility, extracted from the data of the main plot (circles) and the magnetotransport studies (squares) of analogous ZnO structures [3–6].

an instability range. The critical angles corresponding to the transition at exactly $\nu = 2$ are plotted on Fig. 3 with big open circles. At $n = 1.8 \times 10^{11}$ cm^{-2}, the Stoner transition around $\nu \approx 2$ occurs even for the normal orientation of the magnetic field (triangle on the plot). At even lower densities, a stable Stoner ferromagnet is formed already at normal magnetic fields since the magneto-PL evolution is smooth around even filling factors. The critical angles strongly depend on the electron density due to the Fermi-liquid renormalization of the spin susceptibility. Its value can be easily extracted from the data on Fig. 3 using Eq. (1). The calculated values of spin susceptibilities for all studied samples are plotted in the inset in Fig. 3 together with the data taken from previous magnetotransport studies of similar ZnO-based heterostructures [3–6]. The agreement between the two sets of data is apparent and both witness the zero-tilt Stoner transition at densities smaller than $\sim 2 \times 10^{11}$ cm^{-2}. Although the phase diagram corresponds to the quantum Hall state $\nu = 2$, these conditions perfectly correlate with transformations at other even filling factors. In addition, the level crossing with index $j = 2$ [from Eq. (1)] was observed for $\nu = 3$ for the sample with density 2.8×10^{11} cm^{-2}. The tilt angles for this second coincidence lie in a very narrow range of $\Theta_2 = 63.5^\circ \pm 0.5^\circ$. This value is consistent with the angle obtained for $\nu = 2$ via Eq. (1). Instabilities at filling factors deviating from $\nu = 3$ are not observed, possibly due to the less-pronounced exchange effects in level crossing at higher filling factors.

An extended view of these phenomena was obtained by means of inelastic light scattering experiments. Here, we expected the probing of collective excitations to reveal the spin properties of the ground state. As reported in the previous study [12], inelastic light scattering signal corresponding to neutral electronic excitations of 2DES can be found in vicinity of its PL recombination lines. The point of interest here is the estimation of appropriate resonance conditions for each Raman spectral line and its further identification. Data obtained in Ref. [12] for zero magnetic field can be utilized to identify the set of intersubband excitations at any given magnetic field simply by tracing the resonances while continuously increasing magnetic field. In the context of the Stoner transition, most actual are the excitations, sensitive to the spin degree of freedom. The direct sensor is an intra-LL spin exciton (SE): collective mode, indicative of a spin arrangement. Irrespective of the interparticle correlations, the energy of the SE is close to pure Zeeman splitting in the long-wavelength case (Larmor's theorem [13]). This property makes the SE trivial for identification. In our structures, this excitation appears in the Raman spectra over the comparatively wide range of laser wavelengths of ~ 9 Å, overlapping with the resonant conditions for an

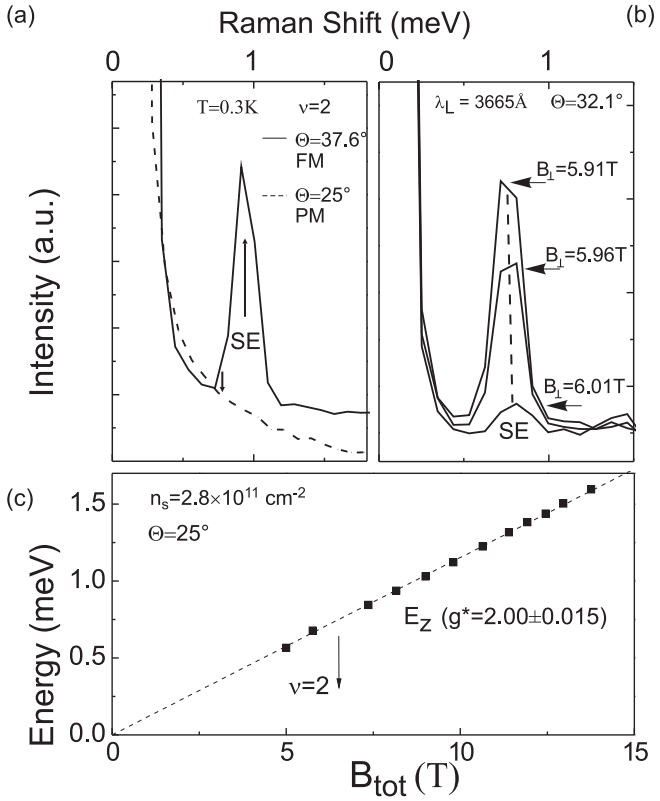

FIG. 4. (a) Raman spectra of spin exciton at $\nu = 2$ and $T = 0.3$ K at two different tilt angles, corresponding to the ferromagnetic and paramagnetic phases (the SE is absent in the PM phase). Arrows indicate the positions of Zeeman energies calculated for both magnetic fields, taking $g^* = 2$. The spectral intensities are normalized to unchanged PL bands (not shown). (b) Spectra of SE at three magnetic fields near the Stoner transition point at $\Theta = 32.1^\circ$, where intensity of SE changes dramatically. (c) Energy of SE measured as a function of the total magnetic field for sample orientation of $\Theta = 25^\circ$.

intra-LL magnetoplasmon. Over a wide span of the magnetic field, the SE energy increases linearly with an effective Lande factor $g^* = 2.00 \pm 0.015$ [plot in Fig. 4(c)]. A feature of interest with regard to this excitation is its most elementary structure with just one quantum number (the total 2DES spin) changed by unity. This hinders the decomposition of the SE into other elementary excitations even when the system deviates from incompressible states. For this reason, the SE is a "long-lived" excitation, and its spectral width in the actual Raman spectra is determined solely by the equipment resolution of ~0.2 meV, rather than its thermal decay and inhomogeneous broadening. The typical SE Raman spectra are given in Figs. 4(a) and 4(b) for filling factors around $\nu = 2$ and different tilt angles.

The most indicative property of the SE is the change in its spectral intensity with change in the spin ordering in the system. According to the trivial spin-flip representation of SE, its weight is obviously proportional to the number of occupied states in the initial spin level and the number of vacancies in the final level. Therefore, the SE should gain the maximum weight in systems with FM ordering and conversely zero weight in the PM phases corresponding to normal states with even filling factors. A quantitative analysis of the SE spectral intensity behavior at arbitrary filling factors is hardly possible since it would require knowledge of the microscopic structure of the ground state and the orbital wave functions of electrons. Nevertheless, the SE line intensity can serve as an indicator of the general asymmetry in the spin-up and -down occupations and is particularly meaningful in the vicinity of integer QH states. In this aspect, the Raman scattering on SE has previously been applied for probing spin polarization in GaAs-based 2DES [14].

Qualitative behavior of SE line intensity near the phase transition is illustrated on Figs. 4(a) and 4(b). For the tilt angle 37.6°, corresponding to the FM phase of $\nu = 2$ the SE line is perfectly visible at the Raman shift equal to Zeeman energy, whereas in the PM phase ($\Theta = 25^\circ$) spin exciton is absent [Fig. 4(a)]. At critical angle $\Theta = 32.1^\circ$ the SE intensity undergoes sharp transformations synchronously with those in magnetophotoluminescence spectra [compare Figs. 4(b) and Fig. 1(d)], what thereby proves the given interpretation of the phases.

Figure 5(a) depicts the magnetic-field dependence of the SE intensity in the sample with density $n_s = 2.8 \times 10^{11}$ cm^{-2} at the four angular orientations matching those of Fig. 1. The horizontal axis represents the normal component of the magnetic field such that the positions of integer filling factors for all angles match each other. We note [in Fig. 5(a), $\Theta = 25^\circ$] that in the ferromagnetic QH state at $\nu = 1$, the intensity reaches a local maximum as per the above-mentioned considerations. Close to $\nu = 2$, the SE spectral weight reduces and abruptly drops to zero over a certain range on both sides of $\nu = 2$. Naturally, in this PM phase with symmetric occupation of the spin-up and -down states, the spin exciton is absent. Spontaneous symmetry breaking occurs around $\nu = 2$ at higher angles, corresponding to the Stoner instability region ($\Theta = 30.8^\circ$ and 32.1° in Fig. 5(a)], though at somewhat different critical filling factors: $\nu^* = 2.01$ and 1.95. Here, the intensity of the SE spectral line dramatically increases and reaches a sharp maximum, thereby indicating the presence of parallel spin alignment in the system. On the right-hand-side region of ν^*, the SE intensity, although it drops dramatically, does not become zero. Therefore, the PM order is not entirely "resumed" there. From the comparison of the SE intensity drop at two critical angles [Figs. 5(a) and 5(b)] one may see that the "purity" of the PM phase at $\nu = \nu^* - 0$ depends on deviation from $\nu = 2$. The residual signal of SE in the PM phase is much lower for $\nu^* = 2.01$, but still nonzero. The reasons for this will be discussed later in the text.

As has been mentioned above, the magnetic-field position of the discontinuity in the SE evolution coincides with that in the magneto-PL dependence. Monitoring of the SE intensity enables explicit characterization of the spin polarization in the two phases. For angles exceeding this instability range, the Stoner transition does not occur; instead, the whole neighborhood of $\nu = 2$ corresponds to the FM phase. The highest tilt angle presented for this sample [Fig. 5(a), $\Theta = 37.6^\circ$] corresponds to smooth evolution both in the PL spectra and Raman spectra of the SE line. A pronounced local maximum in the SE intensity is observed right at $\nu = 2$, evidencing FM ordering of the 2DES. Apart from this feature, we can also notice a qualitatively similar behavior of the SE on the higher-magnetic-field side of ν^* at all angles.

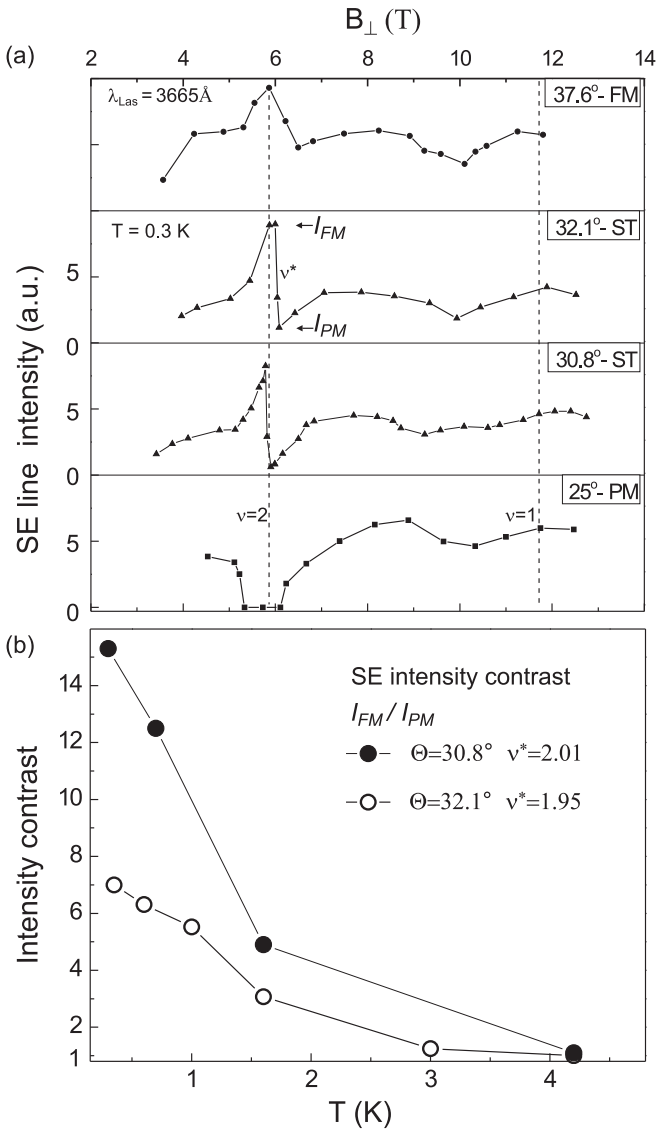

FIG. 5. Behavior of intra-Landau-level spin exciton spectral intensity as a function of the spin transformations at $\nu \approx 2$ in the sample with $n_s = 2.8 \times 10^{11}$ cm^{-2}. (a) The magnetic-field dependence of the SE spectral intensity as recorded for four different tilt angles. In the paramagnetic (PM) phase ($\Theta = 25^\circ$), the SE is absent near $\nu = 2$, in the ferromagnetic (FM) phase ($\Theta = 37.6^\circ$), its intensity exhibits a local maximum, and at the Stoner transition point ($\Theta = 32.1^\circ$ and 30.8°), the SE behavior sharply switches between the PM and FM cases. Note, the Stoner transition at $\Theta = 32.1^\circ$ occurs at somewhat deviated filling factor $\nu^* = 1.95$. In all cases, the SE spectral intensity reaches maximum again in the QHF state of $\nu = 1$. (b) The temperature dependencies of the SE line intensity ratio on either side of the critical magnetic field, recorded at angles $\Theta = 32.1^\circ$ and 30.8°.

The dramatic change in SE intensity across the Stoner transition point can be considered as an indicator of a phase contrast between PM and FM orderings. The thermal stability of these phases was next probed in terms of the "smearing" of the SE intensity collapse. At a fixed tilt angle and varying temperatures, the intensity contrast $I_{\mathrm{FM}} / I_{\mathrm{PM}}$ was calculated as the ratio of the SE intensities corresponding to the local maximum (FM phase) and the local minimum (PM phase) near $\nu = \nu^*$ [see marks on the Fig. 5(a)]. The evolution of this value was measured in the temperature range 0.3–4.2 K for both critical angles from Fig. 5(a). Despite the difference in absolute values [see Fig. 5(b)], in both cases the intensity contrast drops with decrement corresponding to $\sim$2 K. Effectively, the temperature $T = 1.6$ K is the last temperature value at which the Stoner-type discontinuity is observed. This result affords an estimate of the Curie temperature for this Ising QHF to be $T_C \sim 2$ K since at higher temperatures the domains are destroyed.

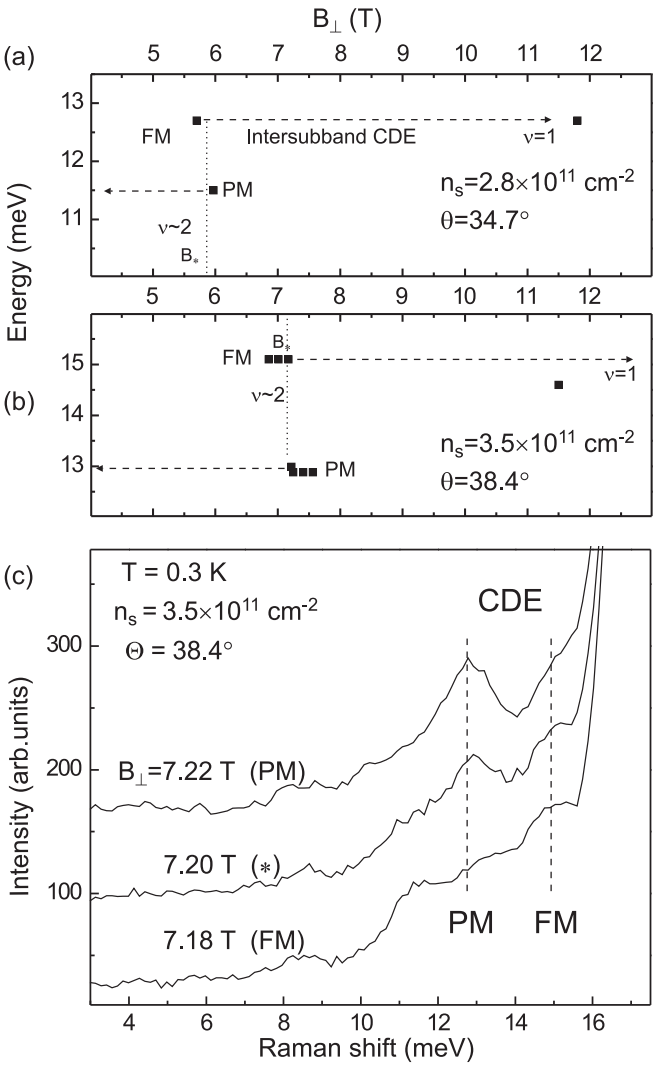

FIG. 6. (a), (b) Energies of intersubband charge density excitation (CDE) measured for two different samples at tilt angles supporting Stoner transition. The sharp energy shift at $\nu \approx 2$ is due to spin rearrangement at the ferromagnetic-paramagnetic (FM-PM) phase transition. Horizontal dashed lines are intended to align CDE energies on either sides of $\nu = 2$ to those of spin-polarized ($\nu = 1$) and spin-unpolarized (zero-magnetic-field) states. (c) Raman spectra of intersubband CDE in the sample with $n_s = 3.5 \times 10^{11}$ cm^{-2} at three closely lying magnetic-field values around the Stoner transition point. The CDE lines at two energy positions are interplayed in intensity according to the phase proportion. Their positions are marked with vertical dashed lines.

An additional tool sensitive to local spin configuration is represented by the energy of the long-wavelength collective excitations. Recently, the intersubband plasmon (or charge density excitation, CDE) has been shown to reflect the spin-polarization degree owing to changes in the exchange energy contribution [15]. Being not particularly susceptible to LL occupation, this intersubband mode nevertheless exhibits a qualitatively different structure between FM and PM spin orderings. A considerable shift in the CDE energy (~1 to 2 meV) has been detected in several ZnO-based structures while continuously tuning the system from an unpolarized $\nu = 2$ state to the FM state $\nu = 1$. In view of our study, the energy shifts of the intersubband CDE at $\nu = 2$ behave in accordance with the spin transformations. First of all, the CDE energy in the $\nu = 2$ PM phase at small tilt angles is equal to that at $B = 0$ T or high-LL filling factors. An identical CDE spectrum is observed on the high-field side of the transition point at tilt angles in the instability range [see the topmost spectrum in Fig. 6(c) and lower-energy data symbols in Figs. 6(a) and 6(b)]. This is clear evidence that the spin-unpolarized states possess intersubband CDE with equal energies. The abrupt shift in the CDE energy occurs while tuning the magnetic field across the transition point [the lowest spectrum in Fig. 6(c)]. This spectrum is identical with that in the neighborhood of $\nu = 2$ at tilt angles lying in the FM region, and most interestingly, it is similar to that of the FM state at $\nu = 1$. This situation is illustrated in Figs. 6(a) and 6(b), corresponding to two samples with different densities. The CDE energies on both sides of the Stoner transition are aligned to those at the FM $\nu = 1$ state (where it is accessible by the solenoid) and $B = 0$ T. Furthermore, the two CDE lines are observed simultaneously in the narrow range of fields across the Stoner transition [the middle spectrum in Fig. 6(c)]. This means that a surface-integrated Raman signal contains the linear superposition of separate spectra from the two phases. This information is valuable since the presence of unperturbed energies of the collective excitations, emanating from the domains of different phases, is possible provided their sizes exceed at least few magnetic lengths. In general, this conclusion agrees with theoretical expectations based on the Ising model [16].

IV. DISCUSSION

The control of the spin configuration at filling factors nearby $\nu = 2$ by means of magnetic-field tilting was shown to differ from the single-particle considerations. So, the phase diagram of Ising QHFs in terms of critical tilt angles contains a wide instability region supporting a phase transition near even filling factors. This implies a substantial exchange contribution in the coincidence condition, which can be fulfilled for a range of filling factors. Qualitatively, this finding agrees with behavior of resistance spikes around integer filling factors at transitions between QHFs, studied earlier in other strongly interacting systems in AlAs [7]. The common conclusion, in particular, is that increasing of the tilt angle results in the downshifting of the critical filling factor. A dramatic dependence of the critical tilt angles on the electron density indicates the Fermi-liquid renormalization of spin susceptibility. Both current optical and previous magnetotransport [3–6] studies of ZnO heterostructures witness that at densities $\sim 2 \times 10^{11}$ cm^{-2} the Stoner transition occurs at normal magnetic-field orientation. This implies that for this density spin susceptibility is enhanced more than threefold with respect to single-particle values. At even lower densities of $\sim 10^{11}$ cm^{-2}, the FM phases are stable independently of the tilt for at least several even filling factors $\nu = 2,4, \ldots$.

The SE line at other even filling factors ($\nu = 4,6, \ldots$) flashes in phase with ferromagnetic order, although its visibility is poorer than that of the FM state $\nu = 2$ due to the stronger laser-line background. A qualitatively similar response was obtained for the phase transition between two spin configurations at $\nu = 3$. In this case, for coincidence angle $\Theta_2 = 63.5^\circ$, the SE intensity drops by a factor of ~2.4 across the transition range of magnetic fields. This value reasonably agrees with naive single-particle picture of spin-state occupation at this filling factor which corresponds to $I_{\max} / I_{\min} = 3$.

The sharp transformations of the QHF phases are particularly amazing, bearing in mind the substantial macroscopic nonuniformity in the electron density. The last estimated to be $\delta n_s \sim 5\%$–10%, depending on the sample. Nevertheless, from the abrupt transformations of PL spectra [Fig. 1(d)] and spin polarization, probed via spin exciton [Fig. 5(a)], we note that the entire transition fits in less than $\delta B \sim 0.1$ T, within ~1.5% of the whole field. The Stoner transition thus appears to be governed by a certain coherent process, aligning a chemical potential level throughout the entire 2DES. The proportion of the two phases is most effectively extracted from the PL-spectra interplay since the PM and FM phases have specific signatures and in addition provide a strong signal. This approach can also aid in characterizing the subtle hysteretic behavior of the Stoner transition at $T = 0.3$ K. So, the sweep-direction difference of the critical magnetic field was of the order 0.01 T for sample 427 with density in the middle of the studied range. The vanishingly small hysteresis is in qualitative agreement with the tiny hysteresis of the magnetoresistance spikes on analogous ZnO structures [4]. This is likely due to the easy-moving domain walls in low-disorder systems.

The nonvanishing SE Raman line on the higher-field side of the transition region corresponds to residual asymmetry in spin occupation despite signs of a dominant PM phase. Even in the most optimal presented case of $\nu^* = 2.01$ for the sample with $n_s = 2.8 \times 10^{11}$ cm^{-2} [see Figs. 5(a) and 5(b)] the residual asymmetry in spin occupations is $\sim \frac{1}{15}$ (as extracted from the SE intensity contrast). There are at least two possible explanations of this perturbed PM phase. The first is thermal nucleation of FM domains, which may be noticeable already at $T = 0.3$ K [according to the fast-decaying dependence on Fig. 5(b)]. The second reason is the electron density fluctuation, which is on the order 5%–10%. In both cases, the proximity to the Stoner transition point should cause smearing of the phase contrast. On deviation from $\nu = 2$, the built-in asymmetry in the spin occupation of the PM phase increases. This causes further smearing of the phase contrast at the transition point (see data for $\nu^* = 1.95$). These effects are, however, too sparse to be discernible in the PL-spectra distortion or modification of the collective CDE mode. The SE is particularly sensitive to perturbations of spin-unpolarized states since its intensity is better traced on a zero background.

The symmetrical situation with nucleation of the minority phase is possible on the ferromagnetic side of the transition point $\nu > \nu^*$. However the SE intensity can hardly serve for detection of this since intensity deviations should have been counted from an unknown maximum intensity level.

The thermal degradation of the SE contrast at a Stoner transition qualitatively shows that domains with rivaling phases undergo melting at temperatures of ∼2 K, which value is significantly lower than Zeeman and exchange energies, but it appears to be comparable with the Curie temperature estimated for an easy-axis QHF in terms of domain-wall excitations [16] $T_C \sim 0.009\, e^2/\varepsilon\ell_B$. This calculation as applied to the sample from Fig. 5 at $\nu = 2$, $B_\perp = 5.8$ T, and $\varepsilon = 8.5$ yields $T_C \sim 1.6$ K. It is also worth noting that at temperatures above 4 K, the behavior of the SE intensity as a function of the magnetic field is absolutely flat, with no peculiarities at integer QH states.

Concerning the domain size, the SE line is of no utility since it reflects a general asymmetry in spin occupation. More indicative of the domain size are the energies of the collective modes. In our study, the observation of intersubband charge density excitations from both phases at a transition point indicates that the QHF domains are substantially large. Their sizes exceed few magnetic lengths since only in that case collective modes may have unperturbed energies. According to theoretical expectations [16], at a transition point (resistance spike maximum in magnetotransport), the typical domain sizes are about dozens of magnetic lengths, but on deviation from the transition point by an effective magnetic field of $\delta B \sim 0.02$ T, the minority phase domains shrink to a size of $\sim 3\,\ell_B$. This result is consistent with our conclusion since at small deviations from the critical magnetic field, the minority phase CDE line vanishes [Fig. 6(c)].

V. CONCLUSION

In conclusion, we performed a magneto-optical study of the Stoner transition between Ising quantum Hall ferromagnetic states in 2D electron systems based in MgZnO/ZnO heterostructures. Abrupt transformations were detected near $\nu = 2,4,6$ both in the photoluminescence spectra and in 2D collective excitations, probed by resonant inelastic light scattering. The transition was facilitated by the tilting of the magnetic field, thus bringing spin Landau levels to coincidence. Depending on the 2D electron density, the spin configuration varied at different critical angles. This phenomenon was exploited to draw the phase diagram for quantum Hall ferromagnets at $\nu = 2$ in terms of the tilt angle vs 2D electron density. Three qualitatively different regions were identified: a stable paramagnetic phase around $\nu = 2$, a stable ferromagnetic phase, and a Stoner instability region in-between. At low electron densities of ~ 1–2×10^{11} cm^{-2}, Fermi-liquid effects lead to a Stoner transition even at normal magnetic-field orientation. The spin configuration at each phase was characterized via the spectral weight of the intra-Landau-level spin exciton. The spin exciton intensity displays a maximumlike behavior in the vicinity of the ferromagnetic states. At a Stoner transition point near $\nu = 2$, it switches from a sharp maximum (in the ferromagnetic phase) to a deep minimum (paramagnetic phase). However, it does not vanish completely, thereby indicating the presence of some ferromagnetic nucleation in the paramagnetic state. From thermal smearing of the SE intensity evolution, the Curie temperature of quantum Hall ferromagnets was estimated to be ∼2 K. Optical signals from the domains were observed to superimpose, which facilitated the direct calculation of the phase proportions across the transition point. It was also shown that at the phase transition point, intersubband collective excitations survive in the domains. They have unperturbed energies, thus indicating that the domain sizes exceed few magnetic lengths.

ACKNOWLEDGMENT

We acknowledge financial support from the Russian Science Foundation (Grant No. 14-12-00693).

[1] J. Falson, Y. Kozuka, J. H. Smet, T. Arima, A. Tsukazaki, and M. Kawasaki, Appl. Phys. Lett. **107**, 082102 (2015).

[2] Y. Kozuka, A. Tsukazaki, and M. Kawasaki, Appl. Phys. Rev. **1**, 011303 (2014).

[3] A. Tsukazaki, A. Ohtomo, M. Kawasaki, S. Akasaka, H. Yuji, K. Tamura, K. Nakahara, T. Tanabe, A. Kamisawa, T. Gokmen *et al.*, Phys. Rev. B **78**, 233308 (2008).

[4] Y. Kozuka, A. Tsukazaki, D. Maryenko, J. Falson, C. Bell, M. Kim, Y. Hikita, H. Y. Hwang, and M. Kawasaki, Phys. Rev. B **85**, 075302 (2012).

[5] D. Maryenko, J. Falson, Y. Kozuka, A. Tsukazaki, and M. Kawasaki, Phys. Rev. B **90**, 245303 (2014).

[6] J. Falson, D. Maryenko, B. Friess, D. Zhang, Y. Kozuka, A. Tsukazaki, J. H. Smet, and M. Kawasaki, Nat. Phys. **11**, 347 (2015).

[7] E. P. De Poortere, E. Tutuc, S. J. Papadakis, and M. Shayegan, Science **290**, 1546 (2000).

[8] E. P. De Poortere, E. Tutuc, and M. Shayegan, Phys. Rev. Lett. **91**, 216802 (2003).

[9] J. Jaroszyński, T. Andrearczyk, G. Karczewski, J. Wróbel, T. Wojtowicz, E. Papis, E. Kamińska, A. Piotrowska, D. Popovic, and T. Dietl, Phys. Rev. Lett. **89**, 266802 (2002).

[10] J. C. Chokomakoua, N. Goel, S. J. Chung, M. B. Santos, J. L. Hicks, M. B. Johnson, and S. Q. Murphy, Phys. Rev. B **69**, 235315 (2004).

[11] V. V. Solovyev, A. B. Van'kov, I. V. Kukushkin, J. Falson, D. Zhang, D. Maryenko, Y. Kozuka, A. Tsukasaki, J. H. Smet, and M. Kawasaki, Appl. Phys. Lett. **106**, 082102 (2015).

[12] A. B. Van'kov, B. D. Kaysin, V. E. Kirpichev, V. V. Solovyev, and I. V. Kukushkin, Phys. Rev. B **94**, 155204 (2016).

[13] M. Dobers, K. von Klitzing, and G. Weimann, Phys. Rev. B **38**, 5453 (1988).

[14] T. D. Rhone, J. Yan, Y. Gallais, A. Pinczuk, L. Pfeiffer, and K. West, Phys. Rev. Lett. **106**, 196805 (2011).

[15] L. V. Kulik, A. B. Van'kov, B. D. Kaysin, and I. V. Kukushkin, Pis'ma Zh. Eksp. Teor. Fiz. **105**, 358 (2017) [JETP Lett. **105**, 380 (2017)].

[16] T. Jungwirth and A. H. MacDonald, Phys. Rev. Lett. **87**, 216801 (2001).